Maghrebian Journal of Pure and Applied Science

ISSN : 2458-715X

http://revues.imist.ma/?journal=mjpas&page=index

https://doi.org/10.48383/IMIST.PRSM/mjpas-v6i2.22927

REVIEW : Synthesis of nanoparticles and nanocomposite of WO_3

C.E. ARVISDEA[1] , K.H. GUSTIAWAN[1*], L. RAMADHANTY[1], N.N. AININ[1], S.W. SARI[1], T. RAHMANIA[1], A.B.D. NANDIYANTO[1]

[1]Departement of Chemistry, Indonesia University of Education, Bandung, Indonesia

***Corresponding Author; Email:** kamelianihg@upi.edu

Received 21 Novembre 2020, Revised 31 January 2021, Accepted 28 February 2021

Abstract. Tungsten oxide (WO_3) is a semiconductor that can be used in a wide variety of applications such as semiconductor gas devices, electronic devices, and photocatalysts. WO_3 can be proposed as a substitute for TiO_2 because it has a narrow bandgap property, which makes this material active in the UV-Vis spectrum. The purpose of writing this paper is to conduct a literature review on the synthesis of WO_3 nanoparticles and nanocomposites using a review method on 50 literature from 2000 to 2020 by reviewing several methods such as hydrothermal methods, sol-gel, low-temperature hydrolysis and, water-in-oil microemulsion in sucrose esters, calcination, flame-assisted spray pyrolysis, ultrasonic, and microwave irradiation. Besides, it is also reviewed based on several starting materials such as sodium tungsten dihydrate, AMT (ammonium metatungsten), ammonium tungstate hydrate, H_2WO_4, phosphotungsten acid, Cl_6W, and W powder.

Keywords: WO_3, Tungsten oxide, Synthesis, Hydrotermal method

I. Introduction

Most of the research in the photocatalytic field has always focused on titanium dioxide (TiO_2). They are cheap, most readily available, thermally and chemically stable, and harmless. However, conventional TiO_2 is only active under UV irradiation [1]. Heterogeneous photocatalysis is the process of forming electron-hole pairs in semiconductor materials by utilizing light energy [2]. As an alternative to the photocatalyst, WO3 is proposed as a substitute for TiO_2, this is because WO_3 can be obtained in various morphological forms such as nanowires, nanosphere, nanoplates and, sub-micron porous balls [3].

WO_3 is a material that is active in the visible light spectrum because of its narrow bandgap. WO_3 is a stable semiconductor material with a narrow bandgap (2.7–3.1 eV) [4]. WO_3 has been found to be very useful in applications of semiconductor gas devices, gas sensors, solar energy devices, electronic devices, photocatalysts, optical storage devices, and emission devices [5,6]. Due to its exotic physico-chemical properties, it shows potential for technological applications in many fields [4] such as in lithium ion batteries [7,8], photocatalysts, and solar energy devices [9]. Tungsten oxide is a material with great potential for use in many practical applications such as electrochromic Smart Glass, switchable devices (screens or mirrors) and, gas sensors (NO_x) [10–13]. WO_3, ZnO and, SnO are widely used in the field of sensor gas applications, in particular, tungsten can detect toxic and dangerous gases such as NO_2, NH_3, acetone [9] carbon monoxide, H_2S, and hydrocarbons such as benzene and methane [14,15]. However, WO_3 is rare, so it is necessary to make it yourself because it will be affected by price increases and export restrictions imposed by producing countries [1].

Several variations of nano tungsten have been produced, such as nanoparticles, nanorods, nanowires, nanosheets and, nanoflowers for the industrial scale, resulting from several methods [9,16] such as sol-gel, electro-deposition, anodization, spray pyrolysis and hydrothermal methods [17–19]. The synthesized particles were characterized using thermogravimetric analysis, X-ray diffraction, nitrogen adsorption, scanning electron microscopy, and transmission electron microscopy (TEM) [20].

Several publications have explained the synthesis of WO_3 as has been done by Parashar et al. [21]. However, even so, the literature that discusses this matter is still limited. Therefore, this study was made to conduct a literature review on the synthesis of WO_3 nanoparticles and nanocomposites using the review method in 50 literature from 2000 to 2020 by reviewing several starting materials such as sodium tungsten dihydrate, AMT (ammonium metatungsten), phosphotungsten acid, H_2WO_4, Cl_6W, and W powder.

2. The proposed approach

2.1 Hydrothermal Method

Many attempts have been made to synthesize one-dimensional nanostructured materials. Based on several methods commonly used for the synthesis of nanomaterials with 1D structures, the hydrothermal method appears to be the right step for the fabrication of anisotropic nanomaterials [22]. The hydrothermal method is of particular interest because of its simplicity, efficiency, high yield and scalability [17,23–25]. WO_3 nanostructures with different crystalline phases and morphology have been synthesized using this technique depending on hydrothermal parameters such as reaction temperature, reaction duration and additives used. This method does not require annealing and high-temperature calcination [26].

Recent studies have proven the fact that WO_3 1D nanostructures such as nanowires, nanobelts, nanorods, nanotubes, nanoribbons and nanofibers produce the best morphology, for these devices their dimensionality limits transport phenomena, large surface to volume ratio, small dimensional ratio to Debye length, and Unique physicochemical properties [27,28] as shown in Figure 1.

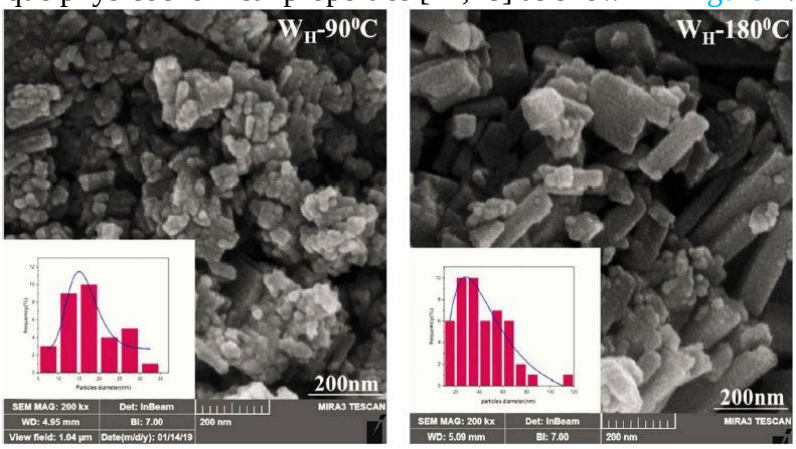

Figure 1. Morphology of WO3 characterized by FESEM. Image adapted from [26]

Na_2WO_4 is used as a starting material in the synthesis of WO_3 nanostructured materials. Na_2WO_4 was dissolved in deionized liquid and then added with a drop of HCl solution drop by drop above the solution while stirring until tungstenic acid formed a precipitate [22]. Impurity is removed by rinsing with deionized liquid and ethanol three times. The washed precipitate was transferred to an oven at 50 ºC for 16 hours to obtain a yellow powder (WS). The product was then calcined at 450 ºC for 1 hour in the air. The solution was then transferred to an autoclave and maintained at 90 ° C for 48 hours. After the reaction is complete, the precipitate is washed with distilled water and ethanol three times, then collected by centrifugation and finally dried at 60 °C for 24 hours [26].

In an experiment conducted by Song et al. [22] before being put into the autoclave, K_2SO_4 was added with various ratios of the precipitate, this was intended to determine the effect of adding organic salts

on the crystallinity and morphology of WO_3 nanostructures. The study results showed that there were differences in the morphology of WO_3 at various amounts of K_2SO_4 used. The samples that did not use K_2SO_4 showed a lamellar structure, while the results of the synthesis with the addition of 15 g of K_2SO_4 showed a mixture of nanorods and nanoparticles, so it can be said that no WO_3 nanowires were formed without the addition of K_2SO_4.

The experiment conducted by Kolhe et al. [29] also used the hydrothermal method but with a few modifications. The main material used is a solution of H_2WO_4 which will then be stirred together with oxalic acid, acetonitrile, urea and HCl solution for 30 minutes. The seed-coated WO_3 FTO substrate was placed into an autoclave filled with a precursor solution that had been prepared and kept at 180 ºC for 6 hours in the oven. After the reaction is complete, the furnace is allowed to naturally cool to room temperature. The FTO substrate was removed from the autoclave, rinsed with ethanol and deionized liquid several times, followed by annealing in air at 500 °C for 2 hours. The study resulted in surface morphology of WO_3 thin films with a monoclinic phase and clear peaks at 807 and 715 cm^{-1}. The thickness of these nanoflakes is in the 50-100 nm range. Nanoflakes of WO_3 are randomly oriented and interconnected, due to the rough surface and porous morphology formed. The nanoflakes have a single crystalline structure with finished lattice edges. The grid spacing was found to be 0.36 nm and readily indexed to the d field distance (002). His research also carried out selectivity against toxic and flammable gases such as SO_2, NH_3, H_2S, and H_2. The WO_3 thin film shows good selectivity to NH3 by providing a maximum response at temperatures of 150 ºC.

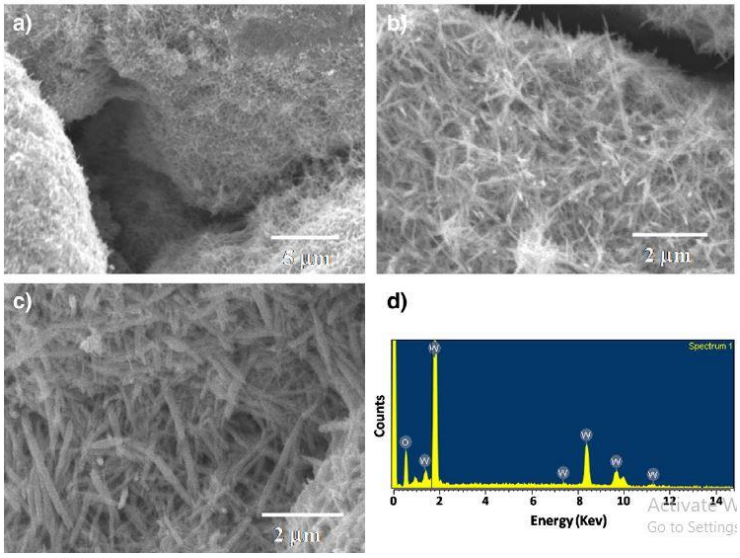

Figure 2. WO_3 nanostructures in SEM with differences with different magnifications: (a) 5000 ×, b) 14,000 × and c) 15,000 × (d) EDS spectrum. Image adapted from [30]

In addition, the experiments conducted by Huirache-Acuña et al. [30] also used a modified hydrothermal method so that it has the name Two-Step Aged Hydrothermal with the first step ammonium metatungstate $[(NH_4)_{10}W_{12}O_{41}xH_2O]$ solution as a source of WO_3 made saturated and acidified with 2.20 N HNO_3 (Normal) to produce a pH of about 5 and then kept in a tightly closed flask under stirring for one week at 60 ° C. Then, 5 mL of the old solution was stored in an autoclave and heated at 200 ° C for 48 hours. The material obtained is filtered and washed with deionized water and dried in the presence of air at room temperature. The composition of the product can be determined by characterization using XRD. The results showed that the XRD pattern results for the WO_3 nanostructures, all reflections were indexed based on hexagonal WO_3 cells; the ratio of the composition of oxygen atom WO3 to tungsten 3: 1 when viewed from the EDS spectrum; irregular and aggregate particles 30-200 nm long and 20-70 nm wide; the Raman band scattering spectroscopy in response to the vibrations of the WO_3 molecules; band position for O_{1s} 530 and 30 eV and W_{4f} 40 and 60 eV, the peak binding energy lies at 35.4 as shown in figure 2. According to the literature, it is WO_3, this means

that the surface of the material contains W^{6+} and not another oxidation number for detected metal. And the growth direction of tungsten oxide nanostructures along the axis with an inter-planar distance of 0.38 nm was detected by HRTEM.

A study with the hydrothermal method was also conducted by Ahmadi et al. [31] on ambient pressure. In this method, three processes are carried out, namely the protonation of the tungstate ion, the crystallization of the tungstite, and the phase transformation into WO3. The first step is the protonation of the tungstate ion on acidification of the solution to form a white solid precipitate:

$$2Na^{+} + [WO_4]^{2-} + 2HCl \rightarrow [WO_2(OH)_2] + 2NaCl$$

The second step is hydration of the tetrahedral molecule $[WO_2(OH)_2]$ and dimerization via an O bridge to form crystals of $[WO(OH)_3\,(H_2O)]_2$(I-O) containing octahedral W-centers by hydrothermal processes in acidic solutions:

$$2[WO_2(OH)_2] + 3H_2O \rightarrow [WO(OH)_3(H_2O)]_2(\mu\text{-O})$$

The third step relates to the dehydration process (i.e., phase transformation):

$$[WO_3.H_2O]n \rightarrow [WO_3]_n + n\text{H2O}$$

The hydrothermal method is also applied in the synthesis process of tungsten oxide quantum dots. First, WO_{3-x} nanoparticles were synthesized by a simple hydrothermal method. In a typical procedure, ammonium tungstate hydrate (1 g), PVP (0.50 g) and ethanoic acid (0.50 g) are dissolved in deionized water with the aid of ultrasonic treatment for 20 minutes. Then, the mixture was transferred into a Teflon-coated autoclave and heated at 180 °C for 12 hours. After that, it was cooled to room temperature, then the product was dialyzed in a 3000 Da dialysis bag against deionized water for 2 days during purification. The resulting light yellow solution was freeze-dried, and a light yellow powder of WO_{3-x}QDs was obtained [32].

The structural characterization of the synthesis results can use the nanosheet mechanism. First, $Na_2WO_2H_2O$ ionized to become WO^{4-}. Then, the WO^{4-} ion will react with the H^{+} from the HCl, forming a H_2WO_4 suspension. The suspension decomposes H_2WO_4, with high temperature and pressure in the hydrothermal process, which results in the nucleation of WO_3. The oleic acid will act as a template and control in the absorption and desorption rates. Then, some of the WO_3 nanosheets are disrelated and form a one-dimensional nano-nano chain. The formation process is described as follows [33]:

$$Na_2WO_4.2H_2O \rightarrow 2Na+ + WO_4^{-} + 2H_2O$$
$$HCl \rightarrow H^{+} + Cl^{-}$$
$$2H^{+} + WO_4^{-} \rightarrow H_2WO_4$$
$$H_2WO_4 \rightarrow WO_3 + H_2$$

2.2 Sol-Gel Method

The sol-gel method is a popular technique for preparing optofunctional materials, such as TiO2 and WO3. Recently, UV irradiation has been incorporated into the sol-gel process, which has shown advantages in the synthesis of functional materials [34]. The sol-gel method is a useful and attractive technique for the preparation of nano-sized particles because of its advantages: good stoichiometric control and production of ultrafine particles with a narrow size distribution in a relatively short processing time at lower temperatures [3]. In addition, mesoporous inorganic materials can be prepared using self-assembled surfactants or block copolymers as internal templates using the sol-gel technique [35]. In this method, the precursor / stabilizer selection ratio and the annealing condition will determine the size of the WO_3 nanoparticles produced [36].

The nano-tungsten oxide structure can also be synthesized using the sol-gel method. The main ingredient is $Na_2WO_4.2H_2O$ which is dissolved in deionized water and added HCl dropwise until the pH reaches 1.50. The solution was stirred for 13 hours, then the impurities were removed by rinsing using deionized water and ethanol three times. The precipitates were transferred to an oven at 50°C for 16 hours to obtain a yellow powder. The powder is calcined at a temperature of 450°C for 1 hour in air [26].

In addition to the synthesis of nanostructures on WO_3, the sol-gel method can also be used for the synthesis of WO_3/TiO_2 composites as was done by Yang et al., [37] which dissolved ten milliliters of $Ti(OBu_4)$ in 10 mL of anhydrous alcohol, and was dispersed ultrasonically to form a mixture. Five milliliters of water are slowly added to the mixture, then stirred for 1 hour at room temperature. Then the addition of a different ammonium tungstate solution was dropped into the mixture according to the amount of WO_3 needed in the WO_3/TiO_2 nanocomposite. The pH value of the solution is kept constant 10. The solution is left to stand for 12 hours at room temperature, followed by filtering, washing several times with deionized water and anhydrous alcohol, drying at 80°C for 12 hours to produce precursors. Calcination of the precursors at 400°C for different hours in air results in the formation of WO_3/TiO_2 nanocomposites.

The results of research conducted by Teoh et al. [38] in synthesizing WO_3/TiO_2 composites using the sol-gel method were that the XRD peak intensity associated with TiO_2 increased gradually with increasing calcination time. Nanocomposites hold promise for high-performance visible light-based photocatalysts. A detailed study of the photocatalytic activity of nanocomposites is ongoing. In the same method L. Liu et al. [35]. Reported that the results obtained from this synthesis in the form of an electrodeposition approach based on electrochemical redox from nanoscale objects can be extended to various transition metal oxide nanoscale objects of various sizes and shapes. Figure 3 shows the variations in film thickness, contrast, staining, and bleaching time as a function of the high deposition potential and interface resistance. Initial bleaching between the surface of the substrate / film causes high inter-surface resistance and inhibits the bleaching of the outer layer of the film. The results show that the thickness and electrochromic performance of WO_3 film can be regulated by time and electrodeposition potential.

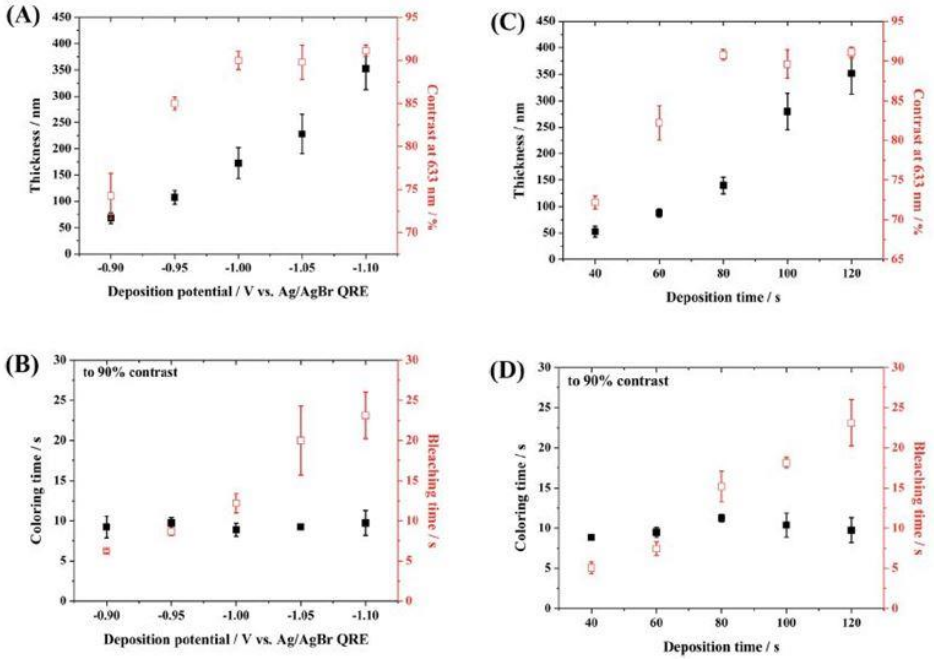

Figure 3. Images (A), (B), (C), and (D) are the effects of deposition potential and time in the WO_3 film. Image adopted from [35]

2.3 Low Temperature Hydrolysis and Chemical Reaction Methode In Water-In-Oil Sucrose Ester Microemulsion

Microemulsion methods have been explored for synthesizing metals, ceramics and polymers. Particles with clear geometries and sizes can be carried out by this synthesis method because all processes are limited in nano-sized droplets (nanoreactors) [34].

In the first method, with or without a microemulsion with a composition: 30 wt.% of S1570, 50 wt.% tetradecane/1-butanol and 20 wt.% aqueous solution containing 4 wt.% tungsten (VI) chloride, stirring vigorously for 2 hours at an ambient temperature of 45°C. Then this solution was stored at 60°C for 4 days and washed several times with deionized water and absolute ethanol to remove surfactants, remaining reactants, and by-products. All precipitates were placed in a furnace at 500°C for 2 hours (hereafter denoted as sample 1).

In the second method, two types of microemulsion without composition: 30 wt.% of S1570, 50 wt.% tetradecane/1-butanol and 20 wt.% aqueous solution were prepared. After stirring and obtaining a homogeneous solution, a microemulsion containing an ammonia solution was added to another microemulsion containing tungsten (VI) chloride. The microemulsion mixture was stirred for 3 hours at about 45°C, then stored at room temperature for 3 days to precipitate. After washing several times with deionized water and absolute ethanol to remove surfactants, residual reactants and by-products, the precipitate was stored in the furnace at 500°C for 2 hours (hereinafter denoted as sample 2).

The CTAB micelle solution used in this study had a composition of 30 wt.% CTAB, 54 wt.% 1-hexanol and 16 wt.% water solution. This composition belongs to the inverted micelle region. For the preparation of WO_3 nanoparticles, two micellar solutions of the above-mentioned composition with aqueous solutions containing 3.10 and 12.50% by weight of tungsten (VI) chloride and ammonia, respectively. After stirring and obtaining a clear solution, micelle solution containing ammonia solution is added to another micelle solution containing tungsten (VI) chloride. The mixed micelle solution was stirred for 4 hours at about 50°C, then kept at room temperature for 3 days to settle. After washing several times with deionized water and absolute ethanol to remove surfactants, residual reactants, and by-products, the precipitate was stored in the furnace at 500°C for 2 hours (denoted as sample 3) [39].

The results obtained in experiments conducted by Asim et al. [39] showed that in their research there was no significant difference between the WO_3 nanoparticles obtained from the use of one sucrose ester microemulsion with a heat aging process and a mixing process of two sucrose ester microemulsions. In both methods using a sucrose ester microemulsion as a template, it is spherical in shape with an orthorhombic lattice and the particle size is roughly between 10 and 50 nm. WO_3 nanoparticles prepared through a CTAB micelle solution are spherical with a larger size range between 25-50 nm and an orthorhombic lattice. Further work to optimize reaction conditions such as precursor concentrations and temperature for all the methods mentioned to prepare smaller size ranges with very narrow size distributions is still ongoing. Finally this study shows that the microemulsion of sucrose ester (biodegradable surfactant) is suitable for synthesizing WO nanoparticles.

2.4 Calcination Method

Calcination is the process of heating, removing water, carbon dioxide or other gases that have bonds with the material at high temperatures below the melting point of the material. In the synthesis process of nano-sized WO_3, the casination method can be carried out using $H_2P_4W_{12}O_{40}{\cdot}xH_2O$ as the main ingredient. $H_2P_4W_{12}O_{40}{\cdot}xH_2O$ is dissolved in water which contains 40% silica particles. The mixture was then stirred for 1 hour and dried in an oven at 80°C to evaporate the solvent. After that, it was calcined at 600°C for 2 hours. The yellow powder formed was then soaked using a hydrofloric acid solution for 3 hours to remove the remaining silicasper. The mixture is then centrifuged and rinsed using distilled water until it reaches a pH of more than 5 and rinsed once using acetone. After that, it was dried in an oven at 100°C for one night [40].

Experiments conducted by Tijani et al. using Spondias Mombin leaf extract has the following work steps; Spondias Mombin leaf extract is added slowly to the ammonium partungstate solution then heated at 120°C while stirring at 150 rpm for 30 minutes. Then slowly added HNO_3 to adjust the pH so that it is in an acidic condition then NH_4OH is added to add the pH to be between 7; 10; and 13. The solution is stirred for 30 minutes and a white precipitate will form. The precipitate is then rinsed using distilled water to remove impurities and then dried at 80°C.

The advantages of the research conducted by Tijani et al. [41] is a reagent that is used environmentally friendly and works specifically, the results obtained in the form of solution pH and calcination temperature play an important role in regulating morphology and structural properties such as average crystal size and surface area. It is known that the crystal size increases with the increase in solution pH and calcination temperature as seen from the XRD peak shown in Figure 4.

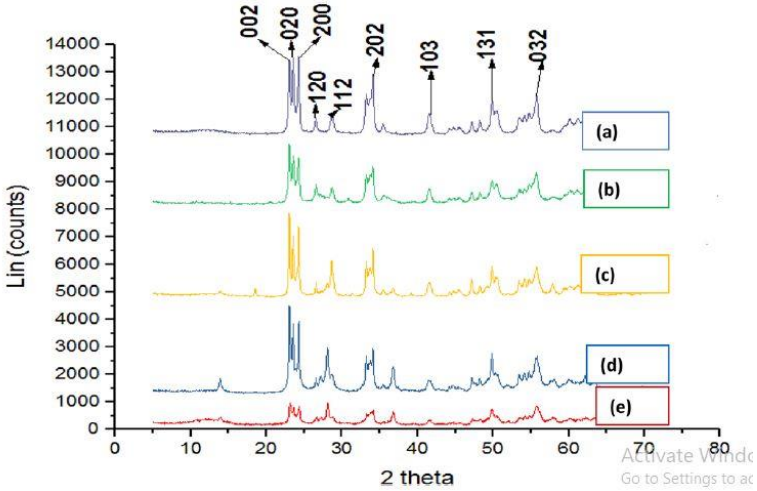

Figure 4. XRD pattern of WO3 nanoparticles with optimization at (a) pH 1, b) pH 4, c) pH 7, d) pH 10, and e) pH 13. The image is adopted [41]

There was no change in the WO_3 phase type at the pH of the applied solution and the calcination temperature, only monoclinic polymorphs were obtained. The acid medium supports the formation of the pure monoclinic symmetry of WO_3.

2.5 Fire-Assisted Spray Pyrolysis Method

Flame synthesis from active nanoparticles can provide access to new structures and materials not available through conventional techniques [42]. To synthesize WO_3/TiO_2 composite nanoparticles, a fire-assisted spray pyrolysis method can be used. Flame technology is a scalable, sustainable and well-established method for the production of large quantities of nanoparticles [38]. This method is effective for producing agglomeration-free particles and has the potential for high-rate production and one-step process applications [43]. Composite nanoparticles were made from precursors containing AMT ($(NH_4)_6(H_2W_{12}O_{I4}\cdot xH_2O)$ as WO_3. The precursors were made by dissolving AMT in DMF, then stirring at 400 rpm at 40 LC. After 40 minutes of mixing, TTIP was added to the precursors and stirring for several minutes. The mass ratio between AMT,TTIP is varied. The precursors are then introduced into the particle production system. The particle production system consists of an ultrasonic nebulizer, a diffuser flame burner, a glass flame reactor, and a filter bag to collect particles. The precursors are first atomized using ultrasonic nebulizer to produce droplets. The resulting droplets are then carried to a diffusion flame burner with nitrogen gas flow at 1 L/min. Methane gas is used as fuel gas with a flow rate of 1 L/min. [1].

The results of experiments conducted by [1] showed that the photocatalytic performance of the WO_3 / TiO_2 nanoparticle composites was higher than the catalyst containing 100% by weight of TiO_2. The effect of mass composition on crystal size, the results are summarized in Table 1.

The increasing number of AMT leads to the production of smaller sized particles. The increase in photocatalytic activity is mainly influenced by the bandgap energy. However, apart from the presence of a band gap, the surface area also plays an important role in changing the photocatalytic activity. Although the current photocatalytic activity is still low, information on the effects of WO_3 and TiO_2 compositions in catalysts opens up new information to create more varied properties for exploratory applications.

Table 1. Effect of Mass Composition on Crystal Size

AMT (wt%)	TTP (wt%)	WO_3 Crystal Size (nm)	TiO_2 Crystal Size (nm)
0	100	-	41
10	90	5.4	39
25	75	5.5	37
55	45	5.7	33
70	30	6	31
100	0	11	-

2.6 Ultrasound Method

Synthesis of TiO_2/WO_3 nanoparticles by Anandan et al. [2] with ultrasonic assistance was carried out in the following steps: About 2.85 mL of titanium isopropoxide was dissolved in 60 mL ethanol. Next, 3.30 g sodium tungstate in 40 mL water was added to the above mixture slowly for 10 minutes at room temperature under an Argon gas atmosphere. In this way, 10 mmol of titanium isoproxide and sodium tungstate are mixed. Then, 0.30 M HNO_3 was added over the top of the mixture and stirred for 10 minutes. The resulting solution was irradiated with a high intensity ultrasonic horn (Ti-horn, 20 kHz, 100 W/cm^2) in the Argon atmosphere for 2.5 hours at room temperature. After sonication, the precipitate was centrifuged and washed using distilled water followed by ethanol several times; then the samples were dried under vacuum at 80^{o}C for about 6 hours. The powder obtained was then calcined at 400^{o}C for 2 hours in air with TiO_2/WO_3 nanoparticles.

The results obtained were the absorbance of TiO_2 /WO_3 nanoparticles located at about 426 nm, a shift of 40 nm compared to TiO_2 (Degussa) nanoparticles (387 nm). The Tauc plot also revealed a nanoparticle band gap of about 2.94 eV. The SEM and TEM images in Figure 5 of the TiO_2 /WO_3 nanoparticles that have been prepared show that the sample consists of mixed particles of square shape, hexagonal diameter of 8-12 nm and the sample crystallizes well. Upon viewing through high resolution TEM (Fig. 5C), it is evidenced that the particles are attached together, making aggregates by sharing between them corners or edges involving probably the formation of Ti–O–W bonds [44,45]. Increasing catalytic activity can be done by increasing the surface area, modifying the structure, morphological properties or producing a new structure. The best way to increase the effectiveness of the catalyst is to modify the surface of the TiO_2 semiconductor with metal. Modification with WO3 is a good form because it can absorb more amounts of OH or H_2O. The preparation of TiO_2 /WO_3 nanocomposites is also advantageous because a small portion of the UV spectrum can be absorbed. In this case it should be noted that the band gap of WO_3 is smaller than that of TiO_2.

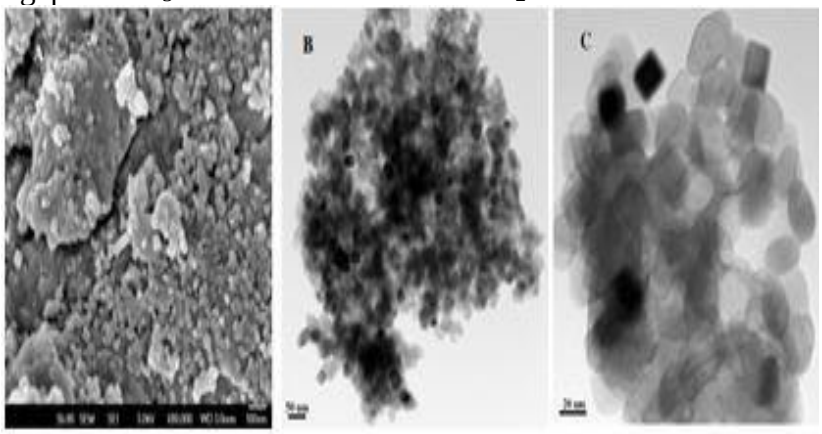

Figure.5. SEM (A) and HRTEM (B,C) from TiO_2/WO_3. Image adopted from [2].

2.7 Microwave Irradiation Method

Tungsten oxide can be hydrated by microwave irradiation methods with and without the using EDTA as surfactant. In this process it takes about 10 minutes with the result of a pale yellow product. The results of XRD powder confirms orthombic phase formation of perovskite such as structures.

The first process, the precursor solution is made by dissolving 2.49 g of tungstat acid (H_2WO_4) in 10 mL of sodium hydroxide (NaOH). It produces a yellow color on a hydrated sodium tungstat solution due to the proton exchange process [46]. Then 0,50 g EDTA (that is 20% tungstat acid weight) added to the precursor solution, acts as surfactant, and several drops of HCl are inserted into the solution. The solution needs to reach the value of pH 1. HCl acts as a deposition substance as well as a medium so that the product has the desired morphology [47]. Approximately 5 mL of double distilled water that is 50 vol.% of the precursor solution is added with the above solution sequentially to respond the microwave quickly. The final solution is presented to the microwave (2.45 GHz) with an optimal power of 180 W for 10 minutes in the air atmosphere. Irradiation is carried out to remove water by drying at 60^{o}C in the air for 1 hour. The process is repeated without adding EDTA salt under the same conditions. Both of that products produce yellow powder that is originalized at 600^{o}C in the air for 6 hours until anhydrous tungsten oxide crystals form [48].

The results of the study conducted by Hariharan et al. [48] showed that in the diffraction results of the powder X-rays confirmed that WO_3. The H_2O that has been prepared respectively is the orthombic phase and $W_{18}O_{49}$ becomes the monoclinical phase. XRD pattern of EDTA assisted $W_{18}O_{49}$ sample contains more number of peaks and they are sharper when compared to that of the sample prepared without surfactant. This is attributed to the fact that the structure variation between WO_3 and WO_2 leads to change in linking of coordination polyhedral from corner sharing to edge sharing [49]. Thus the presence of EDTA enhances the crystallinity and reduces the oxygen content of the end product. The transmission electron micrograph (TEM) in Figure 6 reveals that the $W_{18}O_{49}$ nano sheet has an average dimension of 250 nm long and a width of about 150 nm that serves as a building block for the formation of the $W_{18}O_{49}$ bundle. In the UV-Vis Diffusion Reflectance Spectroscopic (DRS) study, the band gap energy was 3.28 and 3.47 eV for WO_3 samples. H_2O and $W_{18}O_{49}$, respectively.

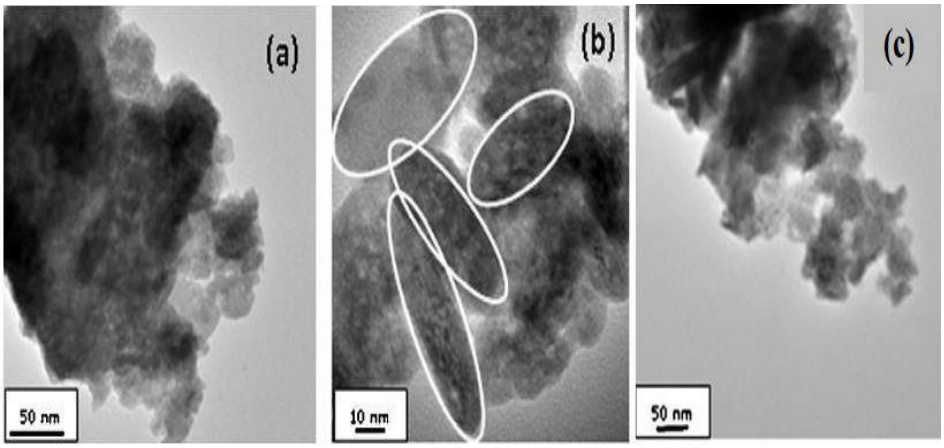

Figure 6. TEM micrograph from $WO_3.H_2O$ is synthesized without adding EDTA (a and b) and synthesized using EDTA (c). Image adopted from the [48]

Based on the literature studies that have been conducted, it can be known that the hydrothermal method is a good method for WO_3 synthesis because the powder is formed directly from the solution, particle size and shape can be controlled using the initial material and different hydrothermal conditions, and the resulting powder is high. Moreover, hydrothermal methods use water solvents to dissolve precursors or recactives so that they are considered more practical and are a fairly abundant common solvent.

Table 2. Material, Research Group, Methods, Results, Advantages, Disadvantages and Refference

Material	Research Group	Methods	Result	Advantages	Disadvantages	Refference
Sodium tungstate hydrate ($Na_2WO_4.2H_2O$)	Jamali and Shariatmadar Tehrani	Sol-gel method and hydrothermal method	Ws Structure and W_{H}-90 hexagonal, W_{H}-450 monoclinic, W_{H}-180 orthorhombic (crystal size increases with calcination and increased synthesis temperature) Morphology of sol-gel sample is in the form of plate particles (after in annealing), and morphology of hydrothermal sample is in the form of rod particles Raman tape scattering spectroscopy korespon to the vibration of WO_3 molecular	Hydrothermal methods are effectively used for the synthesis of 1D WO_3 because solubility increases with increased temperature followed by increased nucleation which will reduce the amount of sodium ions surrounding each nucleus.	The growth mechanisms in plate particles and particle rod WO_3 nanostructures cannot be explained	Jamali and Shariatmadar Tehrani, 2020
	Anandan, S., et al.	Ultrasound method	Nanopartikel TiO_2 / WO_3 menunjukkan pita energi gap sekitar 2.94 eV Electrons can be injected into WO_3 which can be used to reduce W(V) becomes W(VI): $W^{6+} + e_{(TiO2)CB} \rightarrow W^{5+}$ Absorbance for TiO_2/WO_3 noparticles is located at approximately 426 nm with red tape shifting by 40 nm compared to TiO2 nanoparticles (Degussa) 387 nm. Degradation of blue methylen (BM) under visible light illumination	This method is appropriate because when the TiO_2 / WO_3 nanoparticles are combined it is possible to absorb a higher number of photons The addition of TiO_2/WO_3 nanoparticles shows faster BM degradation under irradiation-looking light compared to TiO_2 nanoparticle particles	Pure TiO_2 limited photokatalithic activity because recombination between photogeneration payloads and low Methyl B adsorption and inhibited desorption	Anandan, S., et al., 2014
	Song et al.	Hydrothermal method with K_2SO_4	The addition of K_2SO_4 is helpful in the process of crystallization and growth of WO_3. nanowires No WO_3 nanowires can form without the presence of K_2SO_4	There is no mention of the advantages in the article	There is no definitive explanation for the synthesis of 1D nano structures with the presence of inorganic salts	Song et al., 2007
	Jin et al.	Thermal oxidation methods, hydrothermal methods, anode electrochemical oxidation method	Sensor which is made of hydrants show sensitivities as high as ~32 35 ppm ethanol at an optimal temperature of 35ºC, and also exhibiting excellent selectivity and stability, respectively, as sensor materials promising for detection of low ethanol concentrations	Potential for C_2H_5OH detection WO_3 sensor displays better sensing properties	Cannot affect crystal texture in final process	Jin et al., 2019
Phosphotungsten Acid $H_{26}N_6O_{40}W_{12}$	Gibot, Pierre., et al.	Calcination method uses silica nanosphere as a reagent	Increasing the silica / tungsten precursor will cause the formation of WO_3 which is smaller and less aggregate.	The calcination method using silica nanosphere as a porous template is suitable for synthesizing WO_3 because silica nanosphere can be	There is no mention of deficiencies in the article	Gibot, Pierre., et al., 2011

				organized to create interstitial spaces.		
Ammonium metatungstate $[(NH_4)_{10}W_{12}O_{41}xH_2O]$	Huraiche-Acuna et al.	Two step-aged hydrothermal method	Hexagonal WO_3 nano structure Irregular and aggregate particles Oxygen ratio:tungsten 3:1 Length 30-200 nm and width 20-70 nm O_{1s} tape position 530,3 eV and W_{4f} 40,6 eV, the top of binding energy is located at 35.4 Direction of growth of nano tungsten oxide structure along axis with inter-planar distance of 0.38 nm	The growth mechanism can be determined by HRTEM There is no filth phase on XRD	Monoclinical formation (807 and 715 cm^{-1}) heksagonal WO_3 not found in Raman spectrum	Huraiche-Acuna et al, 2009
	Yang., et al.	Sol-Gel method	The XRD peak intensity associated with TiO_2 increased gradually with increasing calcination time. The addition of WO_3 involve a decrease in the C-axis parameters on the TiO_2, which also increases with the increased calcination time. These nanocomposites hold promise for high-performance visible light-based photocatalysts. A detailed study of the photoalytic activity of nanocompoposit is on going.	WO_3/TiO_2 nanocomposites have been successfully created with the sol-gel method. These nano composites promise to be high-performance visible light-based photo catalysts.	There is no mention of deficiencies in the article	Yang., et al., 2005
	Arutanti et al.	A flame assisted spray pyrolysis	Total AMT (from 0 to 25 wt%) has shown a significant impact on photocatalytic performance The photocatalytic performance of WO_3 / TiO_2 nanoparticle composites is higher than catalysts containing 100% by weight of TiO_2	This method is effective to produce agglomeration free particles and has the potential high production rates and one-step process applications The chemical conversion product is free of impurities The WO_3 conduction band, when TiO2 is present, is suitable for enabling the transfer of photogenerated electrons and the phenomenon of charge separation The combination of these materials is able to reduce the total cost of production because this composite material is low cost than the price of pure WO_3 material (the price of TiO_2 is inexpensive than WO_3)	An increase the amount of AMT aim to production of smaller particles Changing the amount of AMT causes changing a different color, which indicates this amount affects the elemental composition of the particles.	Arutanti et al., 2014
	Tijani et al.	Calsination method using *Spondias mombin* extract	Sample of plants has a higher number of polyphenols can function as an environmentally stabilizer, reducing agent and barrier in the synthesis of WO_3 nanoparticles.	The reagent used is not toxic, enviromentally friendly and specific	There is no mention on the article	Tijani et al., 2019

H_2WO_4	Kolhe et al.	Hydrothermal method and conductrimetry method	The thickness of nanoflakes WO3 in the range of 50-100 nm. The WO_3 thin of layer show a good selectivity NH_3 by providing a maximum response at temperatures of 150C	Good purity and no impurity Increasing the morphology of WO3 thin films can increase the sensitivity of the sensor NH_3 gas	There is no mention on the article	Kolhe et al., 2020
Cl_6W	Asim ., et al.	Hydrolysis with low temprature and microemulsion water-in-fat sucrose esters	This research shown that the microemulsion of sucrose ester (biodegradable surfactant) is suitable for synthesizing WO_3 nanoparticles.	WO_3 nanoparticles prepared through a CTAB micelle solution are spherical with a larger size range between 25-50 nm and an orthorhombic lattice.	These appears to be no significant difference between the WO_3 nanoparticles obtained from the use of one sucrose ester microemulsion with a heat aging process and a mixing process of two sucrose ester microemulsions.	Asim et al., 2006
W powder (Merck)	Liang Lu, dkk. 2014	Metode sol-gel	The thickness and electrochromic performance of the WO3 film can be regulated by the time and electrodeposition potential	Morphological pores can easily experience electrolyte penetration in the film, leading to the surface of the active area. Nanostructures can facilitate intercalation / deintercalation of Li + ions compared to large crystals obtained by sintering Dispersion water of the crystalline WO3 nanoparticles is stabilized by electrostatic repulsion, free of surfactants. This prevents the surfactant remaining in the film The layer with mechanism in electrodeposition is based on the high conductivity of the reduced WO_3 nanoparticles, inherently ensuring good electro-contact and low resistance between nanoparticles Crystal structure provides higher stability in the dye-bleaching cycle compared to amorphous films	Repeated dip-coating or spin-coating, which is poor contact between the layers and consequently is stored	L. Liu et al., 2014

3. Conclusion

Based on several methods used to synthesize WO_3 and WO_3 nanocomposites from various types of available materials, such as sodium tungsten dihydrate, AMT (ammonium metatungsten), Phosphotungsten Acid, H_2WO_4, Cl_6W, and W powder (Merck). The most efficient and effective method is the hydrothermal method because the heating process of the reactants is carried out in a closed container so that the pressure and temperature can increase rapidly. In addition, it produces less impurities when compared to other methods. It can be concluded that the hydrothermal method is inexpensive and more efficient.

References

1. O. Arutanti, A.B.D. Nandiyanto, T. Ogi, F. Iskandar, T.O. Kim, K. Okuyama, Synthesis of composite WO3/TiO2 nanoparticles by flame-assisted spray pyrolysis and their photocatalytic activity, *J. Alloys Compd.* 591 (2014) 121–126. https://doi.org/10.1016/j.jallcom.2013.12.218.
2. S. Anandan, T. Sivasankar, T. Lana-Villarreal, Synthesis of TiO2/WO3 nanoparticles via sonochemical approach for the photocatalytic degradation of methylene blue under visible light illumination, *Ultrason. Sonochem*. 21 (2014) 1964–1968. https://doi.org/10.1016/j.ultsonch.2014.02.015.
3. Y. Gui, J. Zhao, W. Wang, J. Tian, M. Zhao, Synthesis of hemispherical WO 3 / graphene nanocomposite by a microwave-assisted hydrothermal method and the gas-sensing properties to triethylamine, *Mater. Lett.* 155 (2015) 4–7. https://doi.org/10.1016/j.matlet.2015.04.100.
4. R. Nagarjuna, S. Challagulla, P. Sahu, S. Roy, R. Ganesan, Polymerizable sol – gel synthesis of nano-crystalline WO 3 and its photocatalytic Cr (VI) reduction under visible light, *Adv. Powder Technol.* 28 (2017) 3265–3273. https://doi.org/10.1016/j.apt.2017.09.030.
5. J.H. Ha, P. Muralidharan, D.K. Kim, Hydrothermal synthesis and characterization of self-assembled h-WO3 nanowires/nanorods using EDTA salts, *J. Alloys Compd*. 475 (2009) 446–451. https://doi.org/10.1016/j.jallcom.2008.07.048.
6. H. Zheng, J.Z. Ou, M.S. Strano, R.B. Kaner, A. Mitchell, K. Kalantar-Zadeh, Nanostructured tungsten oxide - Properties, synthesis, and applications, *Adv. Funct. Mater*. 21 (2011) 2175–2196. https://doi.org/10.1002/adfm.201002477.
7. S. Komaba, N. Kumagai, K. Kato, H. Yashiro, Hydrothermal synthesis of hexagonal tungsten trioxide from Li 2 WO 4 solution and electrochemical lithium intercalation into the oxide, Solid State Ionics. 135 (2000) 193–197.
8. S. Salmaoui, F. Sediri, N. Gharbi, C. Perruchot, S. Aeiyach, I.A. Rutkowska, P.J. Kulesza, M. Jouini, Hexagonal nanorods of tungsten trioxide: Synthesis, structure, electrochemical properties and activity as supporting material in electrocatalysis, *Appl. Surf. Sci*. 257 (2011) 8223–8229. https://doi.org/10.1016/j.apsusc.2011.04.077.
9. J. Li, X. Liu, J. Cui, J. Sun, Hydrothermal synthesis of self-assembled hierarchical tungsten oxides hollow spheres and their gas sensing properties, ACS Appl. *Mater. Interfaces*. 7 (2015) 10108–10114. https://doi.org/10.1021/am508121p.
10. A. Boudiba, C. Zhang, C. Bittencourt, P. Umek, Hydrothermal synthesis of two dimensional WO 3 nanostructures for NO 2 detection in the ppb-level, *Procedia Eng*. 47 (2012) 228–231. https://doi.org/10.1016/j.proeng.2012.09.125.
11. Y. Hattori, S. Nomura, S. Mukasa, H. Toyota, T. Inoue, Synthesis of tungsten trioxide nanoparticles by microwave plasma in liquid and analysis of physical properties, *J. Alloys Compd*. 560 (2013) 105–110. https://doi.org/10.1016/j.jallcom.2013.01.137.

12. G. Leftheriotis, S. Papaefthimiou, P. Yianoulis, A. Siokou, D. Kefalas, Structural and electrochemical properties of opaque sol-gel deposited WO 3 layers, *Appl. Surf. Sci*. 218 (2003) 276–281.
https://doi.org/10.1016/S0169-4332(03)00616-0.
13.A. Tasaso, P. Ngaotrakanwiwat, Synthesis of Nano-WO 3 Particles with Polyethylene Glycol for Chromic Film, *Elsevier B.V.*, 2015.
https://doi.org/10.1016/j.egypro.2015.11.546.
14. L. Wang, H. Hu, J. Xu, S. Zhu, A. Ding, C. Deng, WO3 nanocubes: Hydrothermal synthesis, growth mechanism, and photocatalytic performance, *J. Mater. Res*. 34 (2019) 2955–2963.
https://doi.org/10.1557/jmr.2019.189.
15. A. Forbes, R.M. Erasmus, Synthesis of tungsten oxide nanostructures by laser pyrolysis Bonex Wakufwa Mwakikunga * Elias Sideras-Haddad and Gift Katumba Bathusile Masina, *Int. J. Nanoparticles*. 1 (2008).
16. R. Hu, H. Wu, K. Hong, Synthesis and characterization of nanocrystalline tungsten oxide nanosheets in large scale, *J. Mater. Res.* 24 (2009) 187–191.
https://doi.org/10.1557/jmr.2009.0026.
17. A.A. Rashid, S. Nor Hayati, C.S.D. Bien, W.Y. Lee, A.S. Muhammad, Preliminary study of WO3 nanostructures produced via facile hydrothermal synthesis process for CO2 sensing, in: *Appl. Mech. Mater*., 2013: pp. 37–41.
https://doi.org/10.4028/www.scientific.net/AMM.431.37.
18. B.T. Sone, J. Sithole, R. Bucher, S.N. Mlondo, J. Ramontja, S.S. Ray, E. Iwuoha, M. Maaza, Synthesis and structural characterization of tungsten trioxide nanoplatelet-containing thin fi lms prepared by Aqueous Chemical Growth ☆, *Thin Solid Films*. 522 (2012) 164–170.
https://doi.org/10.1016/j.tsf.2012.08.032.
19. T. Zhu, M.N. Chong, Y.W. Phuan, J.D. Ocon, E.S. Chan, Effects of electrodeposition synthesis parameters on the photoactivity of nanostructured tungsten trioxide thin films: Optimisation study using response surface methodology, *J. Taiwan Inst. Chem. Eng*. 61 (2016) 196–204.
https://doi.org/10.1016/j.jtice.2015.12.010.
20. A.B.D. Nandiyanto, O. Arutanti, T. Ogi, F. Iskandar, T.O. Kim, K. Okuyama, Synthesis of spherical macroporous WO3 particles and their high photocatalytic performance, *Chem. Eng. Sci*. 101 (2013) 523–532.
https://doi.org/10.1016/j.ces.2013.06.049.
21. M. Parashar, V. Kumar, S. Ranbir, Metal oxides nanoparticles via sol – gel method : a review on synthesis , characterization and applications, *J. Mater. Sci. Mater. Electron*. (2020).
https://doi.org/10.1007/s10854-020-02994-8.
22. X.C. Song, Y.F. Zheng, E. Yang, Y. Wang, Large-scale hydrothermal synthesis of WO3 nanowires in the presence of K_2SO_4, *Mater. Lett*. 61 (2007) 3904–3908.
https://doi.org/10.1016/j.matlet.2006.12.055.
23. R. Esparza, A. Aguilar, A. Escobedo-Morales, C. Patiño-Carachure, U. Pal, G. Rosas, R. Pérez, Synthesis of ZnO_2 nanocrystals produced by hydrothermal process, in: Mater. Res. Soc. *Symp. Proc*., 2010. 97–102.
24. M. V Santhosh, K.S. Devaky, M.K. Jayaraj, Materials Today : Proceedings Hydrothermal synthesis of WO 3 nanoparticles : Characterization and sonocatalytic study, *Mater. Today Proc*. 25 (2020) 183–185.
https://doi.org/10.1016/j.matpr.2019.12.418.
25. S. Cao, H. Chen, Nanorods assembled hierarchical urchin-like WO 3 nanostructures : Hydrothermal synthesis , characterization , and their gas sensing properties, *J. Alloys Compd*. 702 (2017) 644–648.
https://doi.org/10.1016/j.jallcom.2017.01.232.
26. M. Jamali, F. Shariatmadar Tehrani, Effect of synthesis route on the structural and morphological

properties of WO3 nanostructures, *Mater. Sci. Semicond. Process*. 107 (2020) 104829. https://doi.org/10.1016/j.mssp.2019.104829.

27. Z. Gu, H. Li, T. Zhai, W. Yang, Y. Xia, Y. Ma, J. Yao, Large-scale synthesis of single-crystal hexagonal tungsten trioxide nanowires and electrochemical lithium intercalation into the nanocrystals, *J. Solid State Chem.* 180 (2007) 98–105. https://doi.org/10.1016/j.jssc.2006.09.020.
28. H. Hassani, E. Marzbanrad, C. Zamani, Effect of hydrothermal duration on synthesis of WO3 nanorods Effect of hydrothermal duration on synthesis of WO 3 nanorods, *J. Mater. Sci. Mater. Electron*. 22 (2011) 1264–1268. https://doi.org/10.1007/s10854-011-0297-x.
29. P.S. Kolhe, P. Mutadak, N. Maiti, K.M. Sonawane, Synthesis of WO3 nanoflakes by hydrothermal route and its gas sensing application, *Sensors Actuators, A Phys.* 304 (2020) 111877. https://doi.org/10.1016/j.sna.2020.111877.
30. R. Huirache-Acuña, F. Paraguay-Delgado, M.A. Albiter, J. Lara-Romero, R. Martínez-Sánchez, Synthesis and characterization of WO3 nanostructures prepared by an aged-hydrothermal method, *Mater. Charact*. 60 (2009) 932–937. https://doi.org/10.1016/j.matchar.2009.03.006.
31. M. Ahmadi, R. Younesi, M.J.F. Guinel, Synthesis of tungsten oxide nanoparticles using a hydrothermal method at ambient pressure, *J. Mater. Res*. 29 (2014) 1424–1430. https://doi.org/10.1557/jmr.2014.155.
32. Q. Liu, C. Hu, X. Wang, Hydrothermal synthesis of oxygen-deficiency tungsten oxide quantum dots with excellent photochromic reversibility, *Appl. Surf. Sci*. 480 (2019) 404–409. https://doi.org/10.1016/j.apsusc.2019.02.097.
33. L. Hu, P. Hu, Y. Chen, Z. Lin, C. Yu, Synthesis and Gas-Sensing Property of Highly Self-assembled Tungsten Oxide Nanosheets, *Orig. Res*. 6 (2018) 38–41.
34. L. Xiong, T. He, Synthesis and characterization of ultrafine tungsten and tungsten oxide nanoparticles by a reverse microemulsion-mediated method, *Chem. Mater*. 18 (2006) 2211–2218. https://doi.org/10.1021/cm052320t.
35. L. Liu, M. Layani, S. Yellinek, A. Kamyshny, H. Ling, P.S. Lee, S. Magdassi, D. Mandler, "Nano to nano" electrodeposition of WO3crystalline nanoparticles for electrochromic coatings, *J. Mater. Chem. A*. 2 (2014) 16224–16229. https://doi.org/10.1039/c4ta03431g.
36. C. Santato, M. Odziemkowski, M. Ulmann, J. Augustynski, Crystallographically oriented mesoporous WO3 films: Synthesis, characterization, and applications, *J. Am. Chem. Soc*. 123 (2001) 10639–10649. https://doi.org/10.1021/ja011315x.
37. H. Yang, R. Shi, K. Zhang, Y. Hu, A. Tang, X. Li, Synthesis of WO3/TiO2 nanocomposites via sol-gel method, *J. Alloys Compd*. 398 (2005) 200–202. https://doi.org/10.1016/j.jallcom.2005.02.002.
38. W.Y. Teoh, R. Amal, L. Mädler, Flame spray pyrolysis: An enabling technology for nanoparticles design and fabrication, *Nanoscale*. 2 (2010) 1324–1347. https://doi.org/10.1039/c0nr00017e.
39. N. Asim, S. Radiman, M.A. bi. Yarmo, Synthesis of WO3 in nanoscale with the usage of sucrose ester microemulsion and CTAB micelle solution, *Mater. Lett*. 61 (2007) 2652–2657. https://doi.org/10.1016/j.matlet.2006.10.014.
40. P. Gibot, M. Comet, L. Vidal, F. Moitrier, F. Lacroix, Y. Suma, F. Schnell, D. Spitzer, Synthesis of WO3 nanoparticles for superthermites by the template method from silica spheres, *Solid State Sci.* 13 (2011) 908–914. https://doi.org/10.1016/j.solidstatesciences.2011.02.018.
41. J.O. Tijani, O. Ugochukwu, L.A. Fadipe, M.T. Bankole, A.S. Abdulkareem, W.D. Roos, One-step

green synthesis of WO 3 nanoparticles using Spondias mombin aqueous extract: effect of solution pH and calcination temperature, *Appl. Phys. A Mater. Sci. Process.* 125 (2019) 0. https://doi.org/10.1007/s00339-019-2450-y.

42. W.J. Stark, S.E. Pratsinis, A. Baiker, Heterogeneous Catalysis by Flame-Made Nanoparticles, Nanosci. Nanotechnol. 56 (2002) 485–489.
43. R. Strobel, A. Baiker, S.E. Pratsinis, Aerosol flame synthesis of catalysts, *Adv. Powder Technol.* 17 (2006) 457–480. https://doi.org/10.1163/156855206778440525.
44. E. Khoo, P.S. Lee, J. Ma, Electrophoretic deposition (EPD) of WO3 nanorods for electrochromic application, *J. Eur. Ceram. Soc*. 30 (2010) 1139–1144. https://doi.org/10.1016/j.jeurceramsoc.2009.05.014.
45. C. Shifu, C. Lei, G. Shen, C. Gengyu, The preparation of coupled WO3/TiO2 photocatalyst by ball milling, *Powder Technol*. 160 (2005) 198–202. https://doi.org/10.1016/j.powtec.2005.08.012.
46. A. Wolcott, T.R. Kuykendall, W. Chen, S. Chen, J.Z. Zhang, Synthesis and characterization of ultrathin WO3 nanodisks utilizing long-chain Poly(ethylene glycol), *J. Phys. Chem. B.* 110 (2006) 25288–25296. https://doi.org/10.1021/jp064777b.
47. T. Jesionowski, Characterization of silicas precipitated from solution of sodium metasilicate and hydrochloric acid in emulsion medium, *Powder Technol*. 127 (2002) 56–65. https://doi.org/10.1016/S0032-5910(02)00093-1.
48. V. Hariharan, M. Parthibavarman, C. Sekar, Synthesis of tungsten oxide (W 18 O 49) nanosheets utilizing EDTA salt by microwave irradiation method, *J. Alloys Compd*. 509 (2011) 4788–4792. https://doi.org/10.1016/j.jallcom.2011.01.159.
49. E. Rödel, In situ bulk structural investigation of Mo5O14-type mixed metal oxide catalysts for partial oxidation reactions, 2006.
50. Z. Jin, P. Hu, W. Xu, J. Zhou, W. Guo, Y. Chen, C. Qiu, Hydrothermal synthesis and gas sensing properties of hybrid WO3 nano-materials using octadecylamine, *J. Alloys Compd*. 785 (2019) 1047–1055. https://doi.org/10.1016/j.jallcom.2019.01.248.